The Umklapp scattering contribution to the electron-electron scattering part of the thermal resistivity in alkali metals

The Umklapp scattering contribution to the electron–electron scattering part of the thermal resistivity in alkali metals

Lena Lundmark

Department of Theoretical Physics, University of Umeå, S-901 87 Umeå, Sweden

Abstract. The electron–electron scattering contribution to the thermal resistivity has been calculated for the alkali metals Na and K for various pressures. We have used an isotropic Fermi-liquid model where we have corrected for the anisotropic scattering in terms of a 'fractional Umklapp scattering' function, Δ, which is calculated using a pseudopotential band structure model. Our calculations give values of Δ that are ~ 100 times larger than the most commonly accepted values. As a result, this correction will give an enhancement of the electron–electron scattering part of the thermal resistivity of $\sim 5\%$ compared with earlier calculations, where the 'fractional Umklapp scattering' function, Δ, is omitted.

1. Introduction

Since Laubitz [1] managed to separate the electron–electron scattering part of the thermal resistivity at high temperatures (above the Debye temperature, Θ_D) from experimental values of the total thermal and electrical resistivity, the interest in improved experiments and a deeper understanding of the electron–electron scattering contribution to the thermal resistivity has increased [2–4]. Simple arguments [2] show that the temperature dependence of the electron–electron scattering part of the thermal resistivity is linear, $W_{ee} = BT$, where B is a constant. Several different theoretical approaches have been made to determine W_{ee}, and they give results of the same order as experiments, all showing a linear temperature dependence [5, 6].

For an isotropic Fermi liquid it is possible to find an expression for the coefficient B by solving the Boltzmann equation exactly [7–10]. MacDonald and Geldart [5] used a modified Fermi-liquid theory, with Hedin's [11] simple GW approximation to describe the electron–electron interaction in alkali metals. Their results for W_{ee}, given at room temperature (which is above Θ_D), are within the experimental limits. We have previously used their model to calculate the pressure dependence of W_{ee} at room temperature [12], neglecting the effect of Umklapp scattering. There are, of course, some uncertainties in Hedin's model itself, which should be investigated, but to be able to compare different electron–electron interaction models within the thermal resistivity we first have to include corrections like the Umklapp scattering in W_{ee}.

This can be taken care of in an approximate way following Lawrence and Wilkins [6], who calculated W_{ee} for the anisotropic case using a variational method.

They managed to separate the effect of Umklapp scattering into the so called Δ function, which they called the 'fractional Umklapp scattering' function. In the same way, the Δ function can also be used to include the anisotropic Umklapp scattering into the Fermi-liquid model of W_{ee}, as explained in [5]. It has been shown [5] that the Umklapp scattering only gives a smaller correction to $W_{ee}(P = 0)$ (of the order of 3–4%), but to do a proper calculation on $W_{ee}(P)$ we still have to investigate corrections like this one, convincing ourselves that they are small even for higher pressures.

In this paper we present calculations on the pressure dependence of the Δ function for Na and K, and we also investigate the effects this correction will have on our earlier calculated results for $W_{ee}(P)$, given in [12]. The calculation of the Δ function requires a pseudopotential band structure model at varying pressures, which will also be described.

We will start in section 2 with a short description of the theoretical models we have used in order to calculate W_{ee} and Δ. The pseudopotential band structure model is described in section 3. Finally the results are presented and discussed in section 4, and we try to draw some conclusions in section 5.

2. The fractional Umklapp scattering function

In this paper we will use the expression of the electron–electron scattering part of the thermal resistivity, W_{ee}, for an isotropic Fermi liquid as given by MacDonald and Geldart [5],

$$W_{ee}(\Delta = 0) = \frac{3}{8} \frac{m^{*4}T}{\pi^2 \hbar^6 k_F^3 H(\lambda)} \langle W(\theta, \phi)(1 - \cos\theta)/\cos(\theta/2)\rangle \tag{1}$$

where $\langle \ldots \rangle$ denotes a surface integral over the spherical Fermi surface, i.e. over the angles θ and ϕ, which describes the relative location of four k vectors (all situated on the Fermi surface) representing the two interacting electrons before and after the scattering event, as explained by e.g. Smith and Jensen [4]. $W(\theta, \phi)$ is the transition probability, m^* is the quasiparticle mass and $H(\lambda)$ is an infinite series that can be approximated to $\approx 1/2$. This expression is exact for an electron gas and has then been modified by also taking account of the positive background, as explained by MacDonald and Geldart [5]. The Δ function can be included in this expression in an approximate way, and we can write the electron–electron scattering part of the thermal resistivity as [5]

$$W_{ee}(\Delta) = W_{ee}(\Delta = 0)(1 + 3\Delta/8)(1 + \Delta/13)(1 + 3\Delta/22)^{-1}. \tag{2}$$

The 'fractional Umklapp scattering' function Δ has been defined by Lawrence and Wilkins [6] as

$$\Delta \equiv \tfrac{1}{4}\langle |v_1 + v_2 - v_3 - v_4|^2 W\rangle \langle |v|^2 W\rangle^{-1}. \tag{3}$$

Here $\langle \ldots \rangle$ is a fourfold integral over the Fermi surfaces (not necessarily spherical) for the four electrons participating in the scattering event. W is the transition probability, depending on the location of the four k vectors representing the four electrons. W is usually not as simple a function as in the isotropic case, described in connection with

(1). $\boldsymbol{v}_i$ is the velocity of electron i, defined as the energy gradient, $\boldsymbol{v}_{\boldsymbol{k}} \equiv (1/\hbar)\boldsymbol{\nabla}_{\boldsymbol{k}}\epsilon_{\boldsymbol{k}}$, as usual. Δ can then be interpreted as a variation of the velocity difference of the electrons over the Fermi surface, weighted by the transition probability W.

The transition probability W is defined through the golden rule

$$W(1,2{\rightarrow}3,4)\rangle = \frac{2\pi}{\hbar}(|\langle k_3, k_4|V(r,r')|k_1, k_2\rangle|^2$$

$$+ \tfrac{1}{2}|\langle k_3, k_4|V(r,r')|k_1, k_2\rangle - \langle k_4, k_3|V(r,r')|k_1, k_2\rangle|^2) \tag{4}$$

which is an average over spin states. 1 is here short for the state $|\boldsymbol{k}_1\rangle$, representing one of the electrons before the scattering. $V(\boldsymbol{r},\boldsymbol{r}')$ is a screened Coulomb potential, describing the electron–electron interaction. In this paper we have chosen the Thomas–Fermi screened Coulomb potential, following the line taken by Lawrence and Wilkins [6]. It is, of course, in principle possible to choose a more realistic effective electron–electron interaction, and we will discuss this possibility later on.

The wavefunctions will be written as a plane-wave expansion

$$|k\rangle = \frac{1}{\sqrt{\Omega}} \sum_i C_i(k) \exp[\mathrm{i}(k + G_i) \cdot r] \tag{5}$$

where $\boldsymbol{G}_i$ is a reciprocal lattice vector. Lawrence and Wilkins [6] used only the first two terms in this expansion. We have chosen in the following to use the expressions developed by MacDonald *et al* [13], who used 19 plane waves in the expansion. The wavefunction is an eigenfunction to a pseudopotential Hamiltonian, which will be described more thoroughly in the next section.

The pseudopotential wavefunctions will then give us the Born approximation of the Thomas–Fermi interaction [13]

$$\langle k_3, k_4|V^{\mathrm{TF}}|k_1, k_2\rangle = \frac{1}{\Omega} \sum_i \delta(k_1 + k_2 + G_i - k_3 - k_4)$$

$$\times \sum_{n,m,m'} \frac{4\pi e^2 C_n^*(k_3)C_{n'}^*(k_4)C_m(k_1)C_{m'}(k_2)}{|k_3 - k_1 + G_n - G_m|^2 + k_{\mathrm{TF}}^2} \tag{6}$$

where n' satisfies $\boldsymbol{G}_{n'} = \boldsymbol{G}_{m'} + \boldsymbol{G}_m - \boldsymbol{G}_n - \boldsymbol{G}_i$ and the sums are over all terms in the plane-wave expansion. The Thomas–Fermi screening wavevector is given by $k_{\mathrm{TF}} = (16/3\pi^2)r_{\mathrm{s}}^{1/2}k_{\mathrm{F}}$, where k_{F} is the free-electron Fermi wavevector. It is now clear from (3), why we call Δ the 'fractional Umklapp scattering' part. It consists of two fourfold integrals over the Fermi surface, which includes a momentum conservation condition from the Dirac delta function in (6) for different reciprocal lattice vectors $\boldsymbol{G}_i$. We can move the sum over the reciprocal lattice vectors $\boldsymbol{G}_i$ outside the integral in the numerator, and calculate the Δ function for each $\boldsymbol{G}_i$-vector separately,

$$\Delta = \sum_i \Delta_i \tag{7}$$

where Δ_i indicates that $\boldsymbol{k}_3 + \boldsymbol{k}_4 - \boldsymbol{k}_1 - \boldsymbol{k}_2 = \boldsymbol{G}_i$ in the numerator. When $\boldsymbol{G}_i = 0$ there is normal scattering, and when $\boldsymbol{G}_i \neq 0$ we have Umklapp scattering.

3. The pseudopotential method

The pseudopotential method has the advantage that we do not have to deal with the core eigenfunctions explicitly. The valence electron eigenfunctions are expanded into plane waves, which makes it possible to calculate the matrix elements of the Thomas–Fermi potential within the Born approximation in a very straightforward manner, as explained in the last section.

We can write the one-electron Schrödinger equation as

$$\left(-\frac{\hbar^2}{2m} \nabla^2 + V_{\mathrm{ps}} \right) |k\rangle = \epsilon_k |k\rangle \tag{8}$$

where $|k\rangle$ is the pseudopotential eigenfunction (5) representing the valence electrons, but not necessarily orthogonal to the core wavefunctions. The pseudopotential is usually a non-local function, $V_{\mathrm{ps}}(r, r')$. The eigenvalues ϵ_k are exact, i.e. they are also eigenvalues to the exact valence wavefunctions, orthogonal to all core wavefunctions. The Schrödinger equation can be solved both empirically and *ab initio*, and some of the commonly used methods are described in [14,15].

The model we use was developed by Srivastava, and is based on his earlier work on semiconductors [16,17]. We are looking for a self-consistent solution to the Schrödinger equation, and for that purpose we will have to solve a set of eigenvalue equations

$$\sum_i \left[\left(\frac{\hbar^2}{2m} |k + G_i|^2 - \epsilon_k \right) \delta_{G_i, G_j} + V_{\mathrm{ps}}(G_i, G_j) \right] C_i(k) = 0 \tag{9}$$

where $C_i(k)$ are the coefficients from the plane-wave expansion (5).

By solving these eigenvalue equations with a suitable screened starting pseudopotential, we get a first approximation for the eigenvalues and coefficients of the eigenfunctions. These are then used in the next iteration.

The starting pseudopotential is then replaced by an effective potential which will be on the form

$$V_{\mathrm{ps}}(q) = v_{\mathrm{ion}}(q)S(q) + V_{\mathrm{H}}(q) + V_{\mathrm{xc}}(q) \tag{10}$$

where $q = G_i - G_j$ and $S(q)$ is the structure factor.

The ion potential used here, $v_{\mathrm{ion}}(q)$, is given by Bachelet *et al* [15]. They have developed a general method to calculate norm-conserving pseudopotentials for atoms, which they present in the form of analytical expressions with the parameters given in table form. Their calculations are for single atoms, but the transferability to other systems, like crystals, is fulfilled through a transferability condition, as described in [15,18], which is characteristic for norm-conserving pseudopotentials.

In (10) we have also included a Hartree potential

$$V_{\mathrm{H}}(q) = 4\pi e^2 \rho(q)/|q|^2 \tag{11}$$

with the charge density given as $\rho(r) = \sum_k |\langle k|k\rangle|^2$ in real space, where the sum is over all occupied states, which is then Fourier transformed. The screening part of the potential consists of an exchange–correlation part as described by Hedin and Lundqvist [19],

$$V_{\mathrm{xc}}(q) = \beta(\rho)V_{\mathrm{x}}(\rho) \tag{12}$$

where the exchange part is given by

$$V_x(q) = -\alpha \frac{3}{2} \left(\frac{3}{\pi} \right)^{1/3} \rho^{1/3}(q) \tag{13}$$

with $\alpha = 2/3$. The correction for the correlation, $\beta(\rho)$, is given in a parametrized form

$$\beta(\rho) = 1 + 0.0368 \left(\frac{3}{4\pi\rho} \right)^{1/3} \ln \left(1 + 21 \left(\frac{4\pi\rho}{3} \right)^{1/3} \right). \tag{14}$$

This effective potential is then added to the starting potential giving a new trial potential of the form $V_{\text{trial}} = CV_{\text{start}} + (1 - C)V_{\text{ps}}$ where the mixing coefficient C is chosen in a suitable way [16]. This new trial potential is then used to solve (9) once again. The whole procedure is then repeated until we get a self-consistent solution. In the procedure toward self-consistency four special k vectors have been used.

We have used this pseudopotential model to calculate eigenvalues and eigenfunctions for Na and K, for k vectors equally spaced in 1/48th of the Brillouin zone. The calculations have been performed for a number of different volumes of the Wigner–Seitz cell, corresponding to different pressures, at room temperature. Both Na and K will then form a BCC structure. The ion potential used in (10) is given in a parametrized form only at zero pressure, and we therefore treat it as a frozen potential.

Sodium in particular is a very simple metal, in the sense that it has an almost spherical Fermi surface. We will assume that the Fermi surface is exactly spherical in the calculation of the Δ function, which makes it sufficient to solve the pseudopotential equations at $k = k_F$, where k_F is the free-electron Fermi wavevector. The eigenfunctions and eigenvalues of the pseudopotential equation have been calculated at 160 equally spaced k points over the spherical Fermi surface in 1/48th of the Brillouin zone for sodium. In the case of potassium we have chosen to calculate the eigenfunctions and eigenvalues at 342 k points equally spaced in the outer part of 1/48th of the Brillouin zone, surrounding the free-electron spherical Fermi surface. It is then possible to calculate the eigenfunctions at the real distorted Fermi surface by using linear interpolation, since the real Fermi surface is only slightly distorted from the spherical one.

We have compared our results for the eigenvalues at some symmetry points, with the band structure calculations we made in connection with the calculation of $W_{ee}(\Delta = 0, P)$ in [12], using the LMTO (linear muffin-tin orbital) method [20]. We have also compared with results for the eigenvalues given by Dagens and Perrot [21] using the APW (augmented plane wave) method, and with calculations made by Ham [22]. The comparison is presented in table 1 for Na and in table 2 for K.

What can be observed is that the Fermi energy is 5–10 % higher with our pseudopotential calculation. The difference is the same even for higher pressures when we compare with the results given by the LMTO method (not shown in the tables). This systematic difference could be due to the small number of k points (four special points) in the irreducible Brillouin zone that is being used in the self-consistency procedure. Increasing the number of k points, would increase the computer time enormously (since we are dealing with matrices of the order of 100 × 100). In the LMTO method this problem never occurs. There we used 285 k points in the irreducible Brillouin zone, and this was made possible through the smaller dimensionality of the

Table 1. The eigenvalues of Na at some symmetry points and the Fermi energy, E_F, calculated by different band structure methods. They are all given in units of Ryd.

	Pseudopotential	LMTO [12]	Ham [22]	APW [17]
Γ_1	0.0	0.0	0.0	0.0
$\Gamma_{25'}$	1.082	1.137	1.028	1.101
$N_{1'}$	0.273	0.292	0.296	0.291
N_1	0.319	0.317	0.313	0.332
P_4	0.418	0.438	0.437	0.434
P_1	0.540	0.533	0.508	0.577
H_{12}	0.565	0.563	0.573	0.558
H_{15}	0.568	0.602	0.579	0.602
E_F	0.260	0.235	0.235	—

Table 2. The eigenvalues of K at some symmetry points and the Fermi energy, E_F, calculated by different band structure methods. They are all given in units of Ryd.

	Pseudopotential	LMTO [12]	Ham [22]	APW [17]
Γ_1	0.0	0.0	0.0	0.0
$\Gamma_{25'}$	—	0.502	0.477	0.545
N_1	0.180	0.189	0.187	0.201
$N_{1'}$	0.199	0.213	0.219	0.212
P_4	0.262	0.273	0.275	0.275
P_1	0.370	0.375	0.356	0.418
H_{12}	0.326	0.280	0.291	0.290
H_{15}	0.378	0.433	0.417	0.432
E_F	0.167	0.159	0.159	—

secular equations being solved (9×9 matrices) [20]. The difference could also be due to the pseudopotential model itself not giving the correct band structures.

The Fermi surface will also be more irregular in the pseudopotential case. This can most easily be seen in the (110) direction (denoted by N), where the Fermi energy is closer to the energy value at the symmetry point. This will lead to a Fermi surface being closer to the Brillouin zone, and consequently differ more from the spherical shape than for the other band structures. The reason for this irregularity is probably the same as for the deviation of the Fermi energy.

## 4. The pressure dependence of Δ and $W_{ee}(\Delta)$

We have calculated the 'fractional Umklapp scattering', $\Delta(P)$, for the alkali metals Na and K in the pressure ranges 0–30 GPa and 0–12 GPa respectively, using the equations described in section 2. We have then included the Δ function into the thermal resistivity, $W_{ee}(\Delta = 0, P)$ (as given in [12]), according to (2). The results are presented in figures 1–3 and we will discuss them independently for Na and K.

4.1. Results for sodium

Sodium is a simple metal to study, since it has an almost spherical Fermi surface. This will be true even for higher pressures (see Lundmark [12]), and we can argue that it
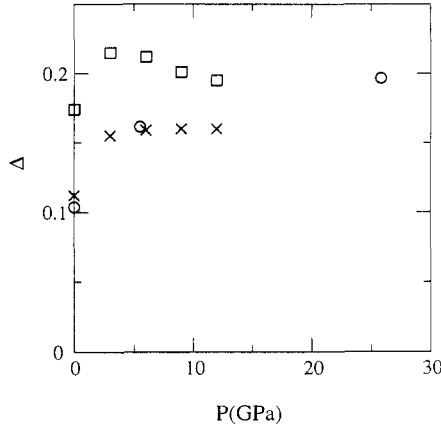
Figure 1. The fractional Umklapp scattering function Δ, given in (3), as a function of pressure. The circles are for sodium, the crosses are for potassium with a spherical Fermi surface and the squares are for potassium with our calculated Fermi surface.
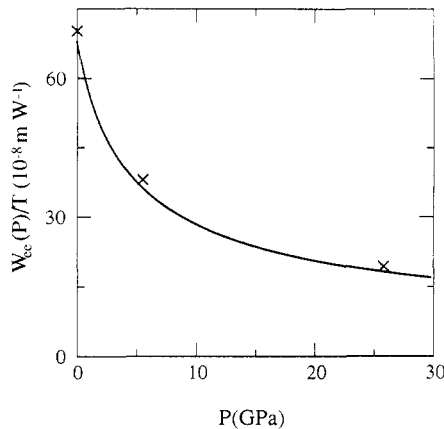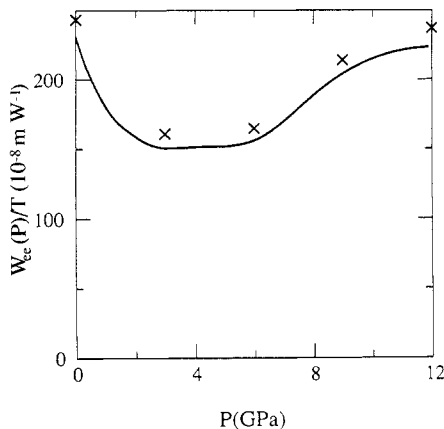

Figure 2. The electron–electron scattering part of the thermal resistivity as a function of pressure for sodium. The full curve is without the fractional Umklapp scattering, $W_{ee}(\Delta = 0)$, as calculated in [12]. The crosses are the corrections when the fractional Umklapp scattering is included, $W_{ee}(\Delta)$ (2).

is a good approximation to work with a completely spherical Fermi surface with a free-electron Fermi wavevector, $k_F = 0.62$ (in units of $2\pi/a$, where a is the length of the BCC unit cell). This will give us a free-electron Fermi energy of $E_F = 0.231$ Ryd at $P = 0$ GPa. We have calculated Δ for three pressures: 0, 5.5 and 26 GPa respectively. Sodium will form a BCC structure in this range, and the equation of state is taken from Aleksandrov *et al* [23].

The Δ function, given in (3), contains two integrals over four k vectors on the Fermi surface. As a result we then have to work with 12-dimensional integrals in the general case. Since we have restricted ourselves to spherical Fermi surfaces, it is possible to reduce the number of dimensions in the integrals to five, as explained by MacDonald *et al* [13]. They are calculated using the Gaussian quadrature method.

Figure 3. The electron–electron scattering part of the thermal resistivity as a function of pressure for potassium. The full curve is without the fractional Umklapp scattering, $W_{ee}(\Delta = 0)$, as calculated in [12]. The crosses are the corrections when the fractional Umklapp scattering is included, $W_{ee}(\Delta)$ (2).

For each term in the summation of the integral we pick out four k vectors on the spherical Fermi surface, representing the two electrons before and after the scattering event. For each k vector we calculate the corresponding eigenfunction from those given in the pseudopotential calculation, by a linear interpolation in three dimensions. The coefficients in the expansion of the eigenfunction in terms of plane waves are then used in the calculation of the Thomas–Fermi matrix elements (6). The k vectors have to fulfil the requirement of conservation of momentum, $k_1 + k_2 + G_i = k_3 + k_4$. This is only possible for the first four shells for a BCC structure, i.e. for the reciprocal lattice vectors that span the first three Brillouin zones and for the case of normal scattering, where $G = (0,0,0)$, as shown by MacDonald et al [13]. For symmetry reasons, all G vectors in the same shell will give an equal contribution to Δ, so we only have to calculate the contribution from each shell once. This will give us four terms in the summation of Δ (7). In practice, we choose three of the k vectors independently in 36 equally spaced directions all over the Fermi surface, and the fourth k vector is then specified by momentum conservation. This will give us a total of 5184 terms summing up for the integrals in Δ_i for each shell or G_i vector.

In the calculation of the matrix elements in (6), we have limited ourselves to 19 terms in the plane-wave expansion of the pseudopotential eigenfunctions (i.e. the first three shells), even though the complete set of plane waves contains 100–200 terms in the self-consistent pseudopotential calculation. We have also performed some tests including 43 terms from the plane-wave expansion in the matrix elements (i.e. including the fourth shell). The change in the Δ function will then be less than 10%, and since the computer time will increase enormously we will settle with 19 terms.

The velocity is defined as the energy gradient on the Fermi surface. We have only solved the pseudopotential eigenvalue equation on the spherical Fermi surface for sodium, which means that we do not have access to the energy gradient. For a local pseudopotential we can calculate the velocity using (9)

$$v_k = \sum_i |C_i(k)|^2 2(k + G_i) \tag{15}$$

given by MacDonald *et al* [13], since the local pseudopotential matrix elements are independent of k. Since sodium has an almost spherical Fermi surface it is a good approximation to assume local pseudopotentials, and use the above expression for the velocity.

The calculated values of Δ are shown in figure (1). Δ is between 0.1 and 0.2, and is increasing with pressure. This is what we could expect, since an increasing pressure will give a more distorted Fermi surface (compared with the free electron case). A spherical Fermi surface will give no contribution to Δ in the normal scattering case, since the velocity difference then equals 0. The more distorted the Fermi surface, the larger velocity difference and consequently the larger Δ will be. When we include Δ in the calculation of $W_{ee}(P)$, according to (2), it will bring about a correction to $W_{ee}(\Delta = 0, P)$ of 3–6%, as shown in figure 2. The only available experimental results so far are for $P = 0$ GPa, and for sodium we have $W_{ee}(P = 0)/T = (110 \pm 60) \times 10^{-8}$ m W^{-1} [24], which is in good agreement with our results.

4.2. Results for K

We have calculated $\Delta(P)$ for five different pressures: 0, 3, 6, 9 and 12 GPa respectively. Potassium forms a BCC structure in this range, with a phase transition at 12 GPa to FCC. The equation of state is taken from Liu [25].

Potassium will also have an almost spherical Fermi surface at atmospheric pressure. But for increasing pressures (i.e. decreasing volume of the unit cell) the Fermi surface will be quite distorted, and for $P = 10$ GPa the Fermi surface in the (110) direction is almost touching the Brillouin zone (see Lundmark [12]). This means that it is no longer a good approximation to assume a spherical Fermi surface.

When the Fermi surface is no longer spherical it is not possible to simplify the 12-dimensional integrals in Δ in the same way as we did for sodium. Nevertheless, we have chosen to proceed from the five-dimensional integrals, but ignoring the exact momentum conservation condition. We start with picking out the k vectors in the same directions as for sodium, fulfilling the momentum conservation. But then we correct their length to equal the length of the true Fermi wavevector in the same direction. It is these k vectors we use to determine the corresponding eigenfunctions to be used in the matrix elements of the Thomas–Fermi potential (6). The differences in the length of the k vectors on the Fermi surface is < 1.5% in the whole pressure range, where the largest differences are in the small surroundings of the symmetry directions. Since the number of k vectors in the symmetry directions is relatively small, we can conclude that the deviations from the momentum conservation in general will be very small.

The pseudopotential eigenvalue equation has been solved for k vectors in the outer part of 1/48th of the Brillouin zone surrounding the free-electron spherical Fermi surface. This makes it possible to use the definition of the velocity as the energy gradient, and calculate the velocity for each k vector on the distorted Fermi surface.

To see how much the non-sphericity will influence the Δ function, we have also calculated $\Delta(P)$ with a spherical free-electron Fermi surface (with $E_F = 0.150$ Ryd at $P = 0$ GPa), in the same way as for sodium. We show the results for the Δ function in figure 1, where we include the calculations with the real distorted Fermi surface and with a spherical free-electron Fermi surface. Since our value of the Fermi energy is probably too high, as discussed in connection with the pseudopotential calculation, we get a Fermi surface that is too large. This indicates that our values of Δ are probably overestimated, and a proper value of Δ should be somewhere between our results and the results given by a spherical free-electron Fermi surface. The values of $\Delta(P)$ for

the spherical free-electron Fermi surface are increasing with pressure, just as in the case of sodium, while the distorted Fermi surface first gives an increasing $\Delta(P)$ which then reaches a maximum and decreases with increasing pressure.

Including our $\Delta(P)$ in the calculation of $W_{ee}(P)$ will give a correction to $W_{ee}(\Delta = 0, P)$ (which is given in [12]), as shown in figure 3. The correction is calculated using (2), and is between 4–5%. We still have the same shape of $W_{ee}(P)$, with a minima between 3 and 6 GPa, as discussed more thoroughly in [12]. The experimental value for potassium at $P = 0$ GPa is $W_{ee}(P = 0)/T = (270 \pm 50) \times 10^{-8}$ m W^{-1} [26]. We can conclude that both our calculated values of $W_{ee}(\Delta = 0, P = 0)$ and $W_{ee}(\Delta, P = 0)$ are within these limits.

4.3. Comparison with other calculations

The fractional Umklapp scattering function, Δ, has been calculated by several authors for different metals. The alkali metals have been delt with by Lawrence and Wilkins [6] and by MacDonald et al [13]. They have both calculated $\Delta(P = 0)$, and we compare their results with ours in table 3.

Table 3. The Δ function as calculated by different authors for $P = 0$ GPa. In the first four columns the same local pseudopotential has been used, given by Ashcroft [29]. In the third and fourth column, we have used 2 and 19 plane waves, respectively. The non-local pseudopotential is described in section 3.

			This paper		
			Local		Non-local
	MTG [13]	LW [6]	2 PW	19 PW	
Na	4.4×10^{-4}	0.015	0.011	0.032	0.104
K	1.6×10^{-3}	0.06	0.044	0.086	0.174

Lawrence and Wilkins [6] are only using two plane waves in their expansion of the pseudo-wavefunction. The first term in the expansion, with $G_i = 0$, is always the dominant one as long as the k vector is well inside the Brillouin zone. Since this is the case for $P = 0$ (with an almost spherical Fermi surface) for both Na and K, they are only keeping the second term in the wavefunction for one of the k vectors in the matrix elements of the Thomas–Fermi potential (6). They also neglect the exchange term in the calculation of the transition probability W, (4), arguing that it will only give a minor contribution. They use a local pseudopotential as given by Ashcroft [29], and calculate the integrals over a spherical Fermi surface. To take account of the reduced number of k vectors that fulfil momentum conservation in the case of Umklapp scattering, they multiply Δ with a factor representing this reduction.

MacDonald *et al* [13] use 19 plane waves in the expansion of the pseudo-wavefunction. They also work with local pseudopotentials given by different authors. To get the coefficients in the plane-wave expansion they solve the eigenvalue equation (9). They integrate over a spherical Fermi surface, where they implicitly reduce the number of possible k vectors in the Umklapp scattering case in an exact manner.

In our calculation of Δ we use the same method as described by MacDonald *et al*. The only difference is that we use a self-consistent, non-local pseudopotential as explained in section 3, making it possible also to include a pressure dependence in the

Δ function. As a test, we have also calculated Δ with the same local pseudopotential [27] as Lawrence and Wilkins and MacDonald *et al*, using both two and 19 plane waves in the pseudo-wavefunction. Since we are using exactly the same equations as MacDonald *et al*, we should get exactly the same results as them with 19 plane waves. The results are given in the fourth column of table 3. It is seen that our values of Δ are a factor of ~ 50 times larger than those given by MacDonald *et al*, and slightly larger than those given by Lawrence and Wilkins. The results with two plane waves (in the third column) give smaller values of Δ than with 19 plane waves, and they are slightly smaller than the results given by Lawrence and Wilkins. MacDonald *et al* argue that including more terms in the plane-wave expansion of the wavefunctions will lower the coefficients in the expansion, and consequently also lower the terms in the matrix elements in (6). The number of terms in the matrix elements is of course increasing, but according to MacDonald *et al* they will add incoherently, ending up with smaller matrix elements, compared with the case of Lawrence and Wilkins. They also argue that Lawrence and Wilkins' approximation for the reduction of the number of available k vectors in the Umklapp scattering case should be lower (~ 3–4 times). These two arguments would then explain why they get much lower values of Δ than Lawrence and Wilkins.

We have not seen this in our calculations. Even though the increasing number of plane waves in the wavefunction expansion inevitably will lower the coefficients, we do not see the same amount of incoherence in adding up the different terms in the matrix elements. The increasing number of terms will instead give us larger matrix elements, ending up with a larger value of Δ. This is most easily seen by comparing the values of Δ with two and 19 plane waves. Since our values with two plane waves are quite close to those given by Lawrence and Wilkins, their approximation for the phase space reduction seems to agree quite well with our calculations. We therefore think that it is still possible that Lawrence and Wilkins approximations are of the right order.

Finally, we should comment on our results for Δ when using a non-local pseudopotential, given in the last column of table 3. They are increasing for both Na and K, compared with the case of a local pseudopotential. This is also what MacDonald *et al* arrived at, and the explanation is that the local pseudopotential is given as the backscattering potential, while the non-local potential generally is much stronger, indicating a stronger electron–electron interaction (cf their figure 3).

4.4. The electron–electron scattering part of the electrical resistivity

Another way of comparing the different calculations of Δ with experiments would be to calculate the electron–electron scattering part of the electrical resistivity, ρ_{ee}. It can be shown [6] that ρ_{ee} is linearly dependent on Δ, and is consequently a much more sensitive function of Δ than W_{ee}. Therefore, we would imagine that a comparison of theoretical and experimental values of ρ_{ee} immediately would tell us at least the magnitude of Δ. Unfortunately, it is not that simple. The electron–electron scattering part of the electrical resistivity is $\sim T^2$ and will only give a minor contribution to the total electrical resistivity. The dominant term is the electron–phonon scattering part, ρ_{ep}. At high temperatures ($T > \Theta_D$), but still far below the Fermi temperature T_F, when the quantization of the phonons is irrelevant, it can be shown that $\rho_{ep} \propto T$ (see Ziman [28]). When the temperature is decreasing so is the electrical resistivity, but its temperature dependence is changed when it is below Θ_D. The contribution from the quantized phonons will instead now give a temperature dependence $\rho_{ep} \propto T^5$. The

electron–electron and electron–phonon scattering part will be of the same size only for very low temperatures, $T \leq 2K$. There is also a contribution from a temperature-independent electron-impurity scattering part, which will dominate in this region, with a size of the order of $10^4 \rho_{ee}$. One therefore needs very accurate measurements at very low temperatures to be able to identify the electron–electron scattering part.

When we calculate the electron–electron scattering part of the electrical resistivity (or of the thermal resistivity) at these low temperatures we also have to take account of a phonon exchange term. This is beyond the scope of this paper, but it has been done by MacDonald *et al* [13], and they argue that the phonon exchange term will dominate over the direct Coulomb electron–electron scattering at low temperatures.

This is not necessarily the case in our calculations. MacDonald *et al* add a phonon-exchange scattering function to the direct Coulomb interaction in the transition probability W in an approximate way, both within $\rho_{ee}/\Delta \sim W_{ee}(\Delta = 0)$ where the transition probability W is given by the Fermi-liquid model, and in the Δ function itself. This will give an enhancement of Δ of a factor of 100 in the case of Na and a factor of 10 in the case of K, which can be seen by comparing the first columns in tables 3 and 4. These new corrected values of Δ are still lower than our values, with only Coulomb scattering included. Therefore we believe that the same kind of correction for the phonon-exchange scattering in our calculations would not give the same drastic increase in Δ.

Table 4. The electron–electron scattering part of the electrical resistivity at $P = 0$ GPa as given by different authors in units of ρ_{ee}/T^2 (10^{-17} Ω m K^{-2}). The values given by [13] and our values are calculated using (16). The experimental values are from [29] for Na and also from [30] for K. MacDonald *et al* [13] have also included a phonon-exchange correction to their values, as explained in the text.

	Δ [13] Phonon-exchange corr.	ρ_{ee}/T^2 [13]	ρ_{ee}/T^2 [6]	ρ_{ee}/T^2 This paper	ρ_{ee}/T^2 Experiment
Na	0.035	140	15	140	180–195
K	0.0207	170	170	600	55–290

We have calculated ρ_{ee} without including the phonon-exchange term, from the expression

$$\rho_{ee} = 0.8 L_0 T W_{ee}(\Delta = 0) \Delta \left(1 + \frac{\Delta}{10.4}\right) \qquad (16)$$

where L_0 is the Lorentz number and $W_{ee}(\Delta = 0)$ is from [12]. The same expression has been used by MacDonald *et al* [13], also including a phonon-exchange term, both in Δ and in $W_{ee}(\Delta = 0)$. The results for ρ_{ee}/T^2 are presented in table 4 and compared with experiment.

5. Conclusions

We have calculated the fractional Umklapp scattering function Δ for Na and K as a function of pressure. The values of $\Delta(P = 0)$ turned out to be ~ 100 times larger than the commonly accepted values given by MacDonald *et al* [13], but of almost the same

order as the values given by Lawrence and Wilkins [6]. We have then inserted this correction into the electron–electron scattering part of the thermal resistivity, W_{ee}. As expected, Δ only has a minor effect on W_{ee}, giving an increase of $\sim 5\%$ in the whole pressure range. The results at $P = 0$ GPa have been compared with experiment, and $W_{ee}(\Delta = 0)$, as well as $W_{ee}(\Delta)$, is within the experimental limits.

In order to improve the results for the electron–electron scattering part of the thermal resistivity we should concentrate on the isotropic part, i.e. $W_{ee}(\Delta = 0)$. We used a Fermi-liquid model to calculate $W_{ee}(\Delta = 0)$, where the electron–electron interaction was formulated in terms of Landau parameters, given by Hedin [11]. He calculated these parameters in the GW approximation using the free-electron Green function and the Coulomb interaction screened with the RPA dielectric function. However, Northrup *et al* [31] have shown that including exchange and correlation in the dielectric function and using a quasiparticle Green function has a very significant effect on the bandwidth of alkali metals and give results in good agreement with experiment. Kukkonen and Smith [32] have arrived at similar conclusions. It would be very interesting to investigate how this improved quasiparticle band structure would affect on the thermal resistivity.

We therefore conclude that a correct description of the electron–electron interaction is the most important part in a theoretical treatment of the electron–electron scattering part of the thermal resistivity.

Acknowledgments

References

[1]   Laubitz M J 1970 *Phys. Rev.* B **2** 2252
[2]   Kaveh M and Wiser N 1984 *Adv. Phys.* **33** 257
[3]   van Vucht R J M, van Kempen H and Wyder P 1985 *Rep. Prog. Phys.* **48** 853
[4]   Smith H and Jensen H H 1989 *Transport Phenomena* (Oxford: Oxford University Press)
[5]   MacDonald A H and Geldart D J W 1980 *J. Phys. F: Met. Phys.* **10** 677
[6]   Lawrence W E and Wilkins J W 1973 *Phys. Rev.* B **7** 2317
[7]   Jensen H H, Smith H and Wilkins J W 1968 *Phys. Lett.* **27A** 532
[8]   Jensen H H, Smith H and Wilkins J W 1969 *Phys. Rev.* **185** 323
[9]   Brooker G A and Sykes J 1968 *Phys. Rev. Lett.* **21** 279
[10] Sykes J and Brooker G A 1970 *Ann. Phys., NY* **56** 1
[11] Hedin L 1965 *Phys. Rev.* **139** A796
[12] Lundmark L 1988 *J. Phys. F: Met. Phys.* **18** 1855
[13] MacDonald A H, Taylor R and Geldart D J W 1981 *Phys. Rev.* B **23** 2718
[14] Heine V 1970 *Solid State Physics* vol 24 (New York: Academic) p 1
      Cohen M L and Heine V 1970 *Solid State Phys.* **24**
[15] Bachelet G B, Hamann D R and Schlüter M 1982 *Phys. Rev.* B **26** 4199
[16] Srivastava G P private communication
[17] Srivastava G P 1982 *J. Phys. C: Solid State Phys.* **15** 707
[18] Topp W C and Hopfield J J 1974 *Phys. Rev.* B **7** 1295
[19] Hedin L and Lundqvist B I 1971 *J. Phys. C: Solid State Phys.* **4** 2064
[20] Skriver H L 1984 *The LMTO Method* (Berlin: Springer)
[21] Dagens L and Perrot F 1973 *Phys. Rev.* B **8** 1281

[22]   Ham F S 1962 *Phys. Rev.* **128** 82

[23]   Aleksandrov I V, Kashinskii V N, Makarenko I N and Stishov S M 1982 *Pis'ma Zh. Eksp. Teor. Fiz.* **36** 336 (Engl. Transl. 1982 *JETP Lett.* **36** 411)

[24]   Cook J G, van der Meer M P and Laubitz M J 1972 *Can. J. Phys.* **50** 1386

[25]   Liu 1986 *J. Phys. Chem. Solids* **47** 1067

[26]   Cook J G 1979 *Can. J. Phys.* **57** 1216

[27]   Ashcroft N W 1968 *J. Phys. Chem.* **1** 232

[28]   Ziman J M 1960 *Electrons and Phonons* (Oxford: Oxford University Press)

[29]   Levy B, Sinvani M and Greenfield A J 1979 *Phys. Rev. Lett.* **43** 1822

[30]   van Kempen H, Lass J S, Ribot J H J M and Wyder P 1976 *Phys. Rev. Lett.* **37** 1574
       Rowlands J A, Duvvury C and Woods S B 1978 *Phys. Rev. Lett.* **40** 1201

[31]   Northrup J E, Hybertsen M S and Louie S G 1987 *Phys. Rev. Lett.* **59** 819

[32]   Kukkonen C A and Smith H 1973 *Phys. Rev. B* **8** 4601